Supporting Information

Effect of water content on thermodynamic properties of compressed hydrogen

Ahmadreza Rahbari,[†] Julio C. Garcia-Navarro,[‡] Mahinder Ramdin,[†] Leo J. P. van den Broeke,[†] Othonas A. Moultos,[†] David Dubbeldam,[¶] and Thijs J. H. Vlugt[*,†]

[†]*Engineering Thermodynamics, Process & Energy Department, Faculty of Mechanical, Maritime and Materials Engineering, Delft University of Technology, Leeghwaterstraat 39, 2628CB, Delft, The Netherlands*

[‡]*HyET Hydrogen BV, Westervoortsedijk 71K, 6827AV Arnhem, The Netherlands*

[¶]*Van't Hoff Institute for Molecular Sciences, University of Amsterdam, Science Park 904, 1098XH Amsterdam, The Netherlands*

E-mail: t.j.h.vlugt@tudelft.nl

S1 Thermodynamic derivatives with respect to β in the NPT ensemble

In this section, we derive an expression for derivative of an extensive property X with respect to β. As stated by Lagache et al.,[1] we show that derivatives with respect to β are independent of the thermal wavelength Λ. We start from the partition function of a mixture of S distinguishable types of monoatomic components[2,3]

$$Q_{N_i,P,T} = \beta P \prod_{i=1}^{S} \frac{1}{\Lambda_i^{3N_i} N_i!} \int \mathrm{d}V V^N \int \mathrm{d}s^N \exp[-\beta \hat{H}(s^N, P, V)] \tag{S1}$$

in which Λ_i is the thermal wavelength of component i, $\beta = 1/(k_\mathrm{B}T)$, k_B is the Boltzmann constant, N_i is the number of molecules of component i, V is the volume, and s are the scaled coordinates. The total number of molecules in the system is denoted by N. The configurational part of enthalpy is defined as $\hat{H}(s^N, P, V) = U(s^N, V) + PV$ in which U is the total interaction energy including both intermolecular (U^ext) and intramolecular (U^int) potential energies, but not the kinetic energy of the system. The thermal wavelength Λ_i of component i is defined as[3]

$$\Lambda_i = \frac{h}{\sqrt{2\pi m_i}} \beta^{1/2} \tag{S2}$$

in which h is the Plank's constant, and m_i is the mass of component i.

Ensemble averages of an extensive property X in the NPT ensemble follow from

$$\langle X \rangle = \frac{\prod_{i=1}^{S} \frac{1}{\Lambda_i^{3N_i} N_i!} \int \mathrm{d}V V^N (X) \int \mathrm{d}s^N \exp[-\beta \hat{H}(s^N, P, V)]}{\prod_{i=1}^{S} \frac{1}{\Lambda_i^{3N_i} N_i!} \int \mathrm{d}V V^N \int \mathrm{d}s^N \exp[-\beta \hat{H}(s^N, P, V)]} \tag{S3}$$

We define a short-hand notation for the denominator:

$$q_{N_i,P,T} = \prod_{i=1}^{S} \frac{1}{\Lambda^{3N_i} N_i!} \int \mathrm{d}V V^N \int \mathrm{d}s^N \exp[-\beta \hat{H}(s^N, P, V)] \tag{S4}$$

To obtain the derivative of $\langle X \rangle$ with respect to β we start from:

$$\left(\frac{\partial \langle X \rangle}{\partial \beta} \right)_P = \frac{\partial}{\partial \beta} \left(\frac{\prod_{i=1}^{S} \frac{1}{\Lambda^{3N_i} N_i!} \int \mathrm{d}V V^N(X) \int \mathrm{d}s^N \exp[-\beta \hat{H}(s^N, P, V)]}{q_{N_i,P,T}} \right)_P \tag{S5}$$

Following the Quotient Rule, we can write

$$\begin{aligned} \left(\frac{\partial \langle X \rangle}{\partial \beta} \right)_P = & \frac{\frac{\partial}{\partial \beta} \left(\prod_{i=1}^{S} \frac{1}{\Lambda^{3N_i} N_i!} \int \mathrm{d}V V^N(X) \exp \int \mathrm{d}s^N \exp[-\beta \hat{H}(s^N, P, V)] \right)_P \times q_{N_i,P,T}}{q_{N_i,P,T}^2} \\ & - \frac{\left(\frac{\partial q_{N_i,P,T}}{\partial \beta} \right)_P}{q_{N_i,P,T}} \times \frac{\prod_{i=1}^{S} \frac{1}{\Lambda^{3N_i} N_i!} \int \mathrm{d}V V^N(X) \int \mathrm{d}s^N \exp[-\beta \hat{H}(s^N, P, V)]}{q_{N_i,P,T}} \end{aligned} \tag{S6}$$

Starting from the first term on the right hand side of Eq. S6, we have

$$\begin{aligned} & \frac{1}{q_{N_i,P,T}} \times \\ & \frac{\partial}{\partial \beta} \left(\prod_{i=1}^{S} \frac{1}{\Lambda^{3N_i} N_i!} \int \mathrm{d}V V^N(X) \exp \int \mathrm{d}s^N \exp[-\beta \hat{H}(s^N, P, V)] \right)_P \\ & = \frac{1}{q_{N_i,P,T}} \times \\ & \left[\frac{\partial}{\partial \beta} \left(\prod_{i=1}^{S} \frac{1}{\Lambda^{3N_i}} \right)_P \times \frac{1}{N_i!} \int \mathrm{d}V V^N(X)] \int \mathrm{d}s^N \exp[-\beta \hat{H}(s^N, P, V)] \right] \\ & \left[+ \prod_{i=1}^{S} \frac{1}{\Lambda^{3N_i} N_i!} \times \frac{\partial}{\partial \beta} \left(\int \mathrm{d}V V^N(X) \int \mathrm{d}s^N \exp[-\beta \hat{H}(s^N, P, V)] \right)_P \right] \end{aligned} \tag{S7}$$

The derivative $\frac{\partial}{\partial\beta}\left(\prod_{i=1}^{S}\frac{1}{\Lambda^{3N_i}}\right)$ in Eq. S7 equals

$$\begin{aligned}
\frac{\partial}{\partial\beta}\left(\prod_{i=1}^{S}\frac{1}{\Lambda^{3N_i}}\right)_P &= \prod_{i=1}^{S}\frac{1}{\left(\frac{h}{\sqrt{2\pi m_i}}\right)^{3N_i}} \times \frac{\partial}{\partial\beta}\left(\prod_{i=1}^{S}\frac{1}{\beta^{3N_i/2}}\right)_P \\
&= \prod_{i=1}^{S}\frac{1}{\left(\frac{h}{\sqrt{2\pi m_i}}\right)^{3N_i}} \times \frac{\partial}{\partial\beta}\left(\beta^{-\frac{3}{2}\sum_{i=1}^{S}N_i}\right)_P \\
&= \prod_{i=1}^{S}\frac{1}{\left(\frac{h}{\sqrt{2\pi m_i}}\right)^{3N_i}} \times \left(-\frac{3}{2}\sum_{i=1}^{S}N_i\beta^{-1-\frac{3}{2}\sum_{i=1}^{S}N_i}\right) \\
&= \prod_{i=1}^{S}\frac{1}{\left(\frac{h}{\sqrt{2\pi m_i}}\right)^{3N_i}} \times \left(-\frac{3}{2\beta}\sum_{i=1}^{S}N_i\prod_{i=1}^{S}\frac{1}{\beta^{3N_i/2}}\right) \\
&= -\frac{3}{2\beta}\sum_{i=1}^{S}N_i\prod_{i=1}^{S}\frac{1}{\Lambda^{3N_i}} \qquad \text{(S8)}
\end{aligned}$$

Combining Eqs. S8 and S9, we have

$$\begin{aligned}
&\frac{1}{q_{N_i,P,T}}\times \\
&\left[\left(-\frac{3}{2\beta}\sum_{i=1}^{S}N_i\right)\prod_{i=1}^{S}\frac{1}{\Lambda^{3N_i}N_i!}\int \mathrm{d}V V^N(X)\int \mathrm{d}s^N \exp[-\beta\hat{H}(s^N,P,V)]\right. \\
&\left.+\prod_{i=1}^{S}\frac{1}{\Lambda^{3N_i}N_i!}\left(\int \mathrm{d}V V^N\left(-X\hat{H}(s^N,P,V)\right)\int \mathrm{d}s^N \exp[-\beta\hat{H}(s^N,V)]\right)\right] \\
&= -\left(\frac{3}{2\beta}\sum_{i=1}^{S}N_i\right)\langle X\rangle - \left\langle X\hat{H}\right\rangle \qquad \text{(S9)}
\end{aligned}$$

The second term on the right hand side of Eq. S6 can be written as:

$$
\begin{aligned}
&-\frac{\left(\frac{\partial q_{N_i,P,T}}{\partial\beta}\right)_P}{q_{N_i,P,T}} \times \frac{\prod_{i=1}^{S}\frac{1}{\Lambda^{3N_i}N_i!}\int \mathrm{d}V V^N(X)\int \mathrm{d}s^N \exp[-\beta\hat{H}(s^N,P,V)]}{q_{N_i,P,T}} \\
&= -\frac{1}{q_{N_i,P,T}}\times \\
&\left[\begin{array}{l} \dfrac{\partial}{\partial\beta}\left(\prod_{i=1}^{S}\dfrac{1}{\Lambda^{3N_i}N_i!}\right)_P \times \int \mathrm{d}V V^N \int \mathrm{d}s^N \exp[-\beta\hat{H}(s^N,P,V)] \\ +\prod_{i=1}^{S}\dfrac{1}{\Lambda^{3N_i}N_i!} \times \dfrac{\partial}{\partial\beta}\left(\int \mathrm{d}V V^N \int \mathrm{d}s^N \exp[-\beta\hat{H}(s^N,P,V)]\right)_P \end{array}\right] \times \langle X\rangle \\
&= -\frac{1}{q_{N_i,P,T}}\times \\
&\left[\begin{array}{l} \left(-\dfrac{3}{2\beta}\sum_{i=1}^{S}N_i\right)\prod_{i=1}^{S}\dfrac{1}{\Lambda^{3N_i}N_i!}\int \mathrm{d}V V^N \int \mathrm{d}s^N \exp[-\beta\hat{H}(s^N,P,V)] \\ +\prod_{i=1}^{S}\dfrac{1}{\Lambda^{3N_i}N_i!}\int \mathrm{d}V V^N \left(-\hat{H}(s^N,P,V)\right)\int \mathrm{d}s^N \exp[-\beta\hat{H}(s^N,P,V)] \end{array}\right] \times \langle X\rangle \\
&= \left(\frac{3}{2\beta}\sum_{i=1}^{S}N_i\right)\langle X\rangle + \langle X\rangle\left\langle\hat{H}\right\rangle
\end{aligned}
\tag{S10}
$$

Combining Eqs. S6, S9 and S10, we have

$$
\begin{aligned}
\left(\frac{\partial\langle X\rangle}{\partial\beta}\right)_P &= \left(\frac{3}{2\beta}\sum_{i=1}^{S}N_i\right)\langle X\rangle + \langle X\rangle\left\langle\hat{H}\right\rangle - \left(\frac{3}{2\beta}\sum_{i=1}^{S}N_i\right)\langle X\rangle - \left\langle X\hat{H}\right\rangle \\
&= \langle X\rangle\left\langle\hat{H}\right\rangle - \left\langle X\hat{H}\right\rangle
\end{aligned}
\tag{S11}
$$

To obtain the derivative of $\langle X\rangle$ with respect to T, one can use the chain rule

$$
\begin{aligned}
\left(\frac{\partial\langle X\rangle}{\partial T}\right)_P &= \left(\frac{\partial\langle X\rangle}{\partial\beta}\right)_P\left(\frac{\partial\beta}{\partial T}\right)_P \\
&= \frac{-1}{k_{\mathrm{B}}T^2}\left(\frac{\partial\langle X\rangle}{\partial\beta}\right)_P
\end{aligned}
\tag{S12}
$$

S2 Thermodynamic derivatives with respect to P in the NPT ensemble

To obtain the derivative of $\langle X \rangle$ with respect to pressure, we start from:

$$\left(\frac{\partial \langle X \rangle}{\partial P}\right)_T = \frac{\partial}{\partial P}\left(\frac{\prod_{i=1}^{S} \frac{1}{\Lambda_i^{3N_i} N_i!} \int \mathrm{d}V V^N(X) \int \mathrm{d}s^N \exp[-\beta \hat{H}(s^N, P, V)]}{q_{N_i,P,T}}\right) \tag{S13}$$

Following the Quotient Rule, we can write

$$\begin{aligned}\left(\frac{\partial \langle X \rangle}{\partial P}\right)_T = & \frac{\frac{\partial}{\partial P}\left(\prod_{i=1}^{S} \frac{1}{\Lambda_i^{3N_i} N_i!} \int \mathrm{d}V V^N(X) \int \mathrm{d}s^N \exp[-\beta \hat{H}(s^N, P, V)]\right)_T \times q_{N_i,P,T}}{q_{N_i,P,T}^2} \\ & - \frac{\left(\frac{\partial q_{N_i,P,T}}{\partial P}\right)_T}{q_{N_i,P,T}} \times \frac{\prod_{i=1}^{S} \frac{1}{\Lambda_i^{3N_i} N_i!} \int \mathrm{d}V V^N(X) \int \mathrm{d}s^N \exp[-\beta \hat{H}(s^N, P, V)]}{q_{N_i,P,T}}\end{aligned} \tag{S14}$$

Starting from the first term on the right hand side of Eq. S14, we have

$$\begin{aligned}& \frac{1}{q_{N_i,P,T}} \times \frac{\partial}{\partial P}\left(\prod_{i=1}^{S} \frac{1}{\Lambda_i^{3N_i} N_i!} \int \mathrm{d}V V^N(X) \int \mathrm{d}s^N \exp[-\beta \hat{H}(s^N, P, V)]\right)_T \\ & = \frac{1}{q_{N_i,P,T}} \times \\ & \left(\begin{array}{l} \prod_{i=1}^{S} \frac{1}{\Lambda_i^{3N_i} N_i!} \int \mathrm{d}V V^N \left(\frac{\partial X}{\partial P}\right)_T \int \mathrm{d}s^N \exp[-\beta \hat{H}(s^N, P, V)] + \\ \prod_{i=1}^{S} \frac{1}{\Lambda_i^{3N_i} N_i!} \int \mathrm{d}V V^N \left(-X\beta \frac{\partial \hat{H}(s^N, P, V)}{\partial P}\right)_T \int \mathrm{d}s^N \exp[-\beta \hat{H}(s^N, P, V)] \end{array}\right)\end{aligned} \tag{S15}$$

The derivative $\left(\frac{\partial \hat{H}(s^N,P,V)}{\partial P}\right)_T$ in Eq. S15 can be written as

$$\begin{aligned}\left(\frac{\partial \hat{H}(s^N,P,V)}{\partial P}\right)_T &= \left(\frac{\partial U(s^N,V)}{\partial P}\right)_T + \left(\frac{\partial (PV)}{\partial P}\right)_T \\ &= V \end{aligned} \tag{S16}$$

As a general case, we assume that X is an extensive variable which may depend on the imposed pressure. A typical example would be $X = \hat{H}$. Combining Eqs. S16 and S37, we have

$$\begin{aligned}&= \frac{1}{q_{N_i,P,T}} \times \\ &\left(\prod_{i=1}^{S} \frac{1}{\Lambda_i^{3N_i} N_i!} \int \mathrm{d}V V^N \left(\frac{\partial X}{\partial P}\right)_T \int \mathrm{d}s^N \exp[-\beta \hat{H}(s^N,P,V)]\right) \\ &\left(\prod_{i=1}^{S} \frac{1}{\Lambda_i^{3N_i} N_i!} \int \mathrm{d}V V^N (-X\beta V) \int \mathrm{d}s^N \exp[-\beta \hat{H}(s^N,P,V)]\right) \\ &= \left\langle \left(\frac{\partial X}{\partial P}\right)_T \right\rangle - \langle X\beta V \rangle \end{aligned} \tag{S17}$$

The second term on the right hand side of Eq. S14 can be written as

$$\begin{aligned}&- \frac{\left(\frac{\partial q_{N_i,P,T}}{\partial P}\right)_T}{q_{N_i,P,T}} \times \frac{\prod_{i=1}^{S} \frac{1}{\Lambda_i^{3N_i} N_i!} \int \mathrm{d}V V^N(X) \int \mathrm{d}s^N \exp[-\beta \hat{H}(s^N,P,V)]}{q_{N_i,P,T}} \\ &= - \frac{\prod_{i=1}^{S} \frac{1}{\Lambda^{3N_i} N_i!} \int \mathrm{d}V V^N \left(-\beta \frac{\partial \hat{H}(s^N,P,V)}{\partial P}\right) \int \mathrm{d}s^N \exp[-\beta \hat{H}(s^N,P,V)]}{q_{N_i,P,T}} \times \langle X \rangle \\ &= \langle X \rangle \langle \beta V \rangle \end{aligned} \tag{S18}$$

Combining Eqs. S14, S17 and S18, we obtain

$$\left(\frac{\partial \langle X \rangle}{\partial P}\right)_T = \beta \left[\langle X \rangle \langle V \rangle - \langle XV \rangle\right] + \left\langle \left(\frac{\partial X}{\partial P}\right)_T \right\rangle \tag{S19}$$

As an example, replacing X with the configurational part of the enthalpy $\hat{H}$ in Eq. S19, we obtain

$$\left(\frac{\partial \left\langle \hat{H} \right\rangle}{\partial P}\right)_T = \beta \left[\left\langle \hat{H} \right\rangle \langle V \rangle - \langle HV \rangle\right] + \langle V \rangle \tag{S20}$$

For the derivative of the internal energy U, the last term in Eq. S19 is zero and we obtain

$$\left(\frac{\partial \langle U \rangle}{\partial P}\right)_T = \beta \left[\langle U \rangle \langle V \rangle - \langle UV \rangle\right] \tag{S21}$$

S3 Computation of solubilities in the liquid and the gas phase

S3.1 The gas phase

The solubility of water in the gas phase is obtained by imposing equal chemical potentials of water in the gas and liquid phases ($\mu_{\mathrm{H_2O_{(l)}}} = \mu_{\mathrm{H_2O_{(g)}}}$):

$$\mu^{\mathrm{id}}_{\mathrm{H_2O_{(g)}}} + \mu^{\mathrm{ex}}_{\mathrm{H_2O_{(g)}}} = \mu_{\mathrm{H_2O_{(l)}}} \tag{S22}$$

and therefore

$$\mu^{\mathrm{id}}_{\mathrm{H_2O_{(g)}}} = \mu_{\mathrm{H_2O_{(l)}}} - \mu^{\mathrm{ex}}_{\mathrm{H_2O_{(g)}}} \tag{S23}$$

Subtracting the reference chemical potential from both sides of Eq. S23 leads to

$$\mu^{\mathrm{id}}_{\mathrm{H_2O_{(g)}}} - \mu^{0}_{\mathrm{H_2O}} = \mu_{\mathrm{H_2O_{(l)}}} - \mu^{\mathrm{ex}}_{\mathrm{H_2O_{(g)}}} - \mu^{0}_{\mathrm{H_2O}} \tag{S24}$$

The first term on the left hand side of Eq. S24 is related to the number density of water in the gas phase (see Eq. 9 from the main text)

$$\mu^{\mathrm{id}}_{\mathrm{H_2O_{(g)}}} - \mu^{0}_{\mathrm{H_2O}} = k_{\mathrm{B}}T \ln\left(\frac{\left\langle \rho_{\mathrm{H_2O_{(g)}}} \right\rangle}{\rho_0}\right) \tag{S25}$$

Combining Eqs. S24 and S25 leads to

$$\frac{\left\langle \rho_{\mathrm{H_2O_{(g)}}} \right\rangle}{\rho_0} = \exp\left[\frac{\mu^{\mathrm{id}}_{\mathrm{H_2O_{(g)}}} - \mu^{0}_{\mathrm{H_2O}}}{k_{\mathrm{B}}T}\right] = \exp\left[\frac{\mu_{\mathrm{H_2O_{(l)}}} - \mu^{\mathrm{ex}}_{\mathrm{H_2O_{(g)}}} - \mu^{0}_{\mathrm{H_2O}}}{k_{\mathrm{B}}T}\right] \tag{S26}$$

S3.2 The liquid phase

The solubility of hydrogen in the liquid phase is obtained by imposing equal chemical potentials of hydrogen in the gas and liquid phases ($\mu_{\mathrm{H_2(g)}} = \mu_{\mathrm{H_2(l)}}$):

$$\mu^{\mathrm{id}}_{\mathrm{H_2(l)}} + \mu^{\mathrm{ex}}_{\mathrm{H_2(l)}} = \mu_{\mathrm{H_2(g)}} \tag{S27}$$

and therefore

$$\mu^{\mathrm{id}}_{\mathrm{H_2(l)}} = \mu_{\mathrm{H_2(g)}} - \mu^{\mathrm{ex}}_{\mathrm{H_2(l)}} \tag{S28}$$

Subtracting the reference chemical potential from both sides leads to

$$\mu^{\mathrm{id}}_{\mathrm{H_2(l)}} - \mu^{0}_{\mathrm{H_2}} = \mu_{\mathrm{H_2(g)}} - \mu^{\mathrm{ex}}_{\mathrm{H_2(l)}} - \mu^{0}_{\mathrm{H_2}} \tag{S29}$$

The first term on the left hand side of Eq. S29 is related to the number density of hydrogen in the liquid phase (see Eq. 9 from the main text)

$$\mu^{\mathrm{id}}_{\mathrm{H_2(l)}} - \mu^{0}_{\mathrm{H_2}} = k_{\mathrm{B}} T \ln\left(\frac{\left\langle \rho_{\mathrm{H_2(l)}} \right\rangle}{\rho_0}\right) \tag{S30}$$

Combining Eqs. S29 and S30 leads to

$$\frac{\left\langle \rho_{\mathrm{H_2(l)}} \right\rangle}{\rho_0} = \exp\left[\frac{\mu^{\mathrm{id}}_{\mathrm{H_2(l)}} - \mu^{0}_{\mathrm{H_2}}}{k_{\mathrm{B}} T}\right] = \exp\left[\frac{\mu_{\mathrm{H_2(g)}} - \mu^{\mathrm{ex}}_{\mathrm{H_2(l)}} - \mu^{0}_{\mathrm{H_2}}}{k_{\mathrm{B}} T}\right] \tag{S31}$$

S4 Freezing-point depression of water-hydrogen mixtures

At the freezing point, the chemical potentials of the liquid phase and the solid phase are equal

$$\mu_{\mathrm{water}}\left(T_{\mathrm{m}}, P_{\mathrm{m}}\right) = \mu_{\mathrm{ice}}\left(T_{\mathrm{m}}, P_{\mathrm{m}}\right) \tag{S32}$$

When hydrogen is dissolved in water, the freezing point temperature changes by ΔT_{f}. For low solubilities of hydrogen in the liquid phase, the activity coefficient of water equals one. The chemical potential of water in a water-hydrogen mixture at the freezing point equals

$$\mu_{\mathrm{water}}\left(T_{\mathrm{m}} + \Delta T_{\mathrm{f}}, P_{\mathrm{m}}\right) + R\left(T_{\mathrm{m}} + \Delta T_{\mathrm{f}}\right) \ln\left(1 - x_{\mathrm{H_2}}\right) = \mu_{\mathrm{ice}}\left(T_{\mathrm{m}} + \Delta T_{\mathrm{f}}, P_{\mathrm{m}}\right) \tag{S33}$$

in which $x_{\mathrm{H_2}}$ is the mole fraction of hydrogen in the liquid phase. We assume that $x_{\mathrm{H_2}}$ is small such that the solution is ideal, and $R\left(T_{\mathrm{m}} + \Delta T_{\mathrm{f}}\right) \approx R T_{\mathrm{m}}$, and $\ln\left(1 - x_{\mathrm{H_2}}\right) \approx -x_{\mathrm{H_2}}$. Rearranging Eq. S33 and dividing by $T_{\mathrm{m}} \Delta T_{\mathrm{f}}$ leads to

$$\frac{\frac{\mu_{\mathrm{water}}(T_{\mathrm{m}}+\Delta T_{\mathrm{f}}, P_{\mathrm{m}}) - \mu_{\mathrm{water}}(T_{\mathrm{m}}, P_{\mathrm{m}})}{T_{\mathrm{m}}}}{\Delta T_{\mathrm{f}}} - \frac{R x_{\mathrm{H_2}}}{\Delta T_{\mathrm{f}}} = \frac{\frac{\mu_{\mathrm{ice}}(T_{\mathrm{m}}+\Delta T_{\mathrm{f}}, P_{\mathrm{m}}) - \mu_{\mathrm{ice}}(T_{\mathrm{m}}, P_{\mathrm{m}})}{T_{\mathrm{m}}}}{\Delta T_{\mathrm{f}}} \tag{S34}$$

For small values of ΔT_{f}, we can write the first term on the left hand side of Eq. S34 as

$$\frac{\frac{\mu_{\mathrm{water}}(T_{\mathrm{m}}+\Delta T_{\mathrm{f}},P_{\mathrm{m}})-\mu_{\mathrm{water}}(T_{\mathrm{m}},P_{\mathrm{m}})}{T_{\mathrm{m}}}}{\Delta T_{\mathrm{f}}} \approx \left(\frac{\partial \frac{\mu_{\mathrm{water}}(T,P_{\mathrm{m}})}{T_{\mathrm{m}}}}{\partial T}\right)_{P_{\mathrm{m}}} \tag{S35}$$

The derivative on the right hand side of Eq. S35 is obtained using the chain rule

$$\begin{aligned}\left(\frac{\partial(\mu_{\mathrm{water}}/T)}{\partial T}\right)_P &= \left(\frac{\partial(\mu_{\mathrm{water}}/T)}{\partial \beta}\right)_P \left(\frac{\partial \beta}{\partial T}\right)_P \\ &= \frac{-1}{k_{\mathrm{B}}T^2}\left(\frac{\partial(\mu_{\mathrm{water}}/T)}{\partial \beta}\right)_P \\ &= \frac{-1}{T^2}\left(\frac{\partial(\beta\mu_{\mathrm{water}})}{\partial \beta}\right)_P\end{aligned} \tag{S36}$$

in which $\beta = 1/(k_{\mathrm{B}}T)$. It is well known that $\left(\frac{\partial(\beta\mu_{\mathrm{water}})}{\partial \beta}\right)_P = \overline{h}_{\mathrm{water}}$ in which $\overline{h}_{\mathrm{water}}$ is the partial molar enthalpy of water.[4,5] Combining Eqs. S35 and S36, we can write

$$\frac{\frac{\mu_{\mathrm{water}}(T_{\mathrm{m}}+\Delta T_{\mathrm{f}},P_{\mathrm{m}})-\mu_{\mathrm{water}}(T_{\mathrm{m}},P_{\mathrm{m}})}{T_{\mathrm{m}}}}{\Delta T_{\mathrm{f}}} \approx -\frac{\overline{h}_{\mathrm{water}}}{T_{\mathrm{m}}^2} \tag{S37}$$

In a similar manner, for ice, we can write

$$\frac{\frac{\mu_{\mathrm{ice}}(T_{\mathrm{m}}+\Delta T_{\mathrm{f}},P_{\mathrm{m}})-\mu_{\mathrm{ice}}(T_{\mathrm{m}},P_{\mathrm{m}})}{T_{\mathrm{m}}}}{\Delta T_{\mathrm{f}}} \approx -\frac{\overline{h}_{\mathrm{ice}}}{T_{\mathrm{m}}^2} \tag{S38}$$

Combining Eqs. S34, S37 and S38 leads to

$$\frac{\overline{h}_{\mathrm{water}}}{T^2} + \frac{R x_{\mathrm{H_2}}}{\Delta T_{\mathrm{f}}} = \frac{\overline{h}_{\mathrm{ice}}}{T^2} \tag{S39}$$

The freezing point depression is obtained by rearranging Eq. S39

$$\Delta T_{\mathrm{f}} = \frac{R T_{\mathrm{m}}^2 x_{\mathrm{H_2}}}{\Delta \overline{h}_{\mathrm{fus}}} \tag{S40}$$

in which $\Delta\overline{h}_{\text{fus}} = \overline{h}_{\text{ice}} - \overline{h}_{\text{water}}$ is the enthalpy of fusion of ice. Eq. S40 is the well-known expression for the melting point depression.[5] The difference between the enthalpy of ice and water is a function of temperature and does not vary significantly with pressure.[6] Osborn and Dickison[6] obtained the enthalpy of fusion $\Delta\overline{h}_{\text{fus}} = 6010.44$ J/mol from experiments. Osborn and Dickison also tabulated the difference in enthalpy between water and ice as a function of temperature. The enthalpy difference between ice and water as a function of temperature is provided in Table S1 of this document.

Table S1: Enthalpy differences between ice and water by Dickinson and Osborn as a function of temperature.[6] The temperature is in units of K, $T_0 = 273.15$ K, and enthalpies are in units of J/mol.

T_{ice}/[K]	Difference in enthalpy		T_{water}/[K]	h_T^{water}-$h_{T_0}^{\text{water}}$
	$h_{T_0}^{\text{ice}} - h_T^{\text{ice}}$	$h_{T_0}^{\text{water}} - h_T^{\text{ice}}$		
244.26	997.3	7006.28	273.15	0.00
245.37	959.6	6968.56	274.26	83.81
246.48	926.1	6935.04	275.37	167.61
247.59	892.5	6901.52	276.48	251.42
248.71	854.8	6863.81	277.59	339.42
249.82	821.3	6830.28	278.71	423.23
250.93	783.6	6792.57	279.82	507.03
252.04	750.1	6759.05	280.93	590.84
253.15	712.4	6721.33	282.04	674.65
254.26	674.6	6683.62	283.15	758.45
255.37	636.9	6645.91	284.26	842.26
256.48	599.2	6608.19	285.37	926.07
257.59	561.5	6570.48	286.48	1009.88
258.71	523.8	6532.77	287.59	1093.68
259.82	486.1	6495.05	288.71	1177.49
260.93	448.4	6457.34	289.82	1261.30
262.04	406.5	6415.44	290.93	1345.10
263.15	368.8	6377.72	292.04	1428.91
264.26	326.8	6335.82	293.15	1512.72
265.37	289.1	6298.11	294.26	1596.53
266.48	247.2	6256.20	295.37	1680.33
267.59	209.5	6218.49	296.48	1764.14
268.71	167.6	6176.59	297.59	1847.95
269.82	125.7	6134.68	298.71	1931.75
270.93	83.8	6092.78	299.82	2015.56
272.04	41.9	6050.88	300.93	2099.37
273.15	0.0	6008.97	302.04	2183.18
			303.15	2266.98
			304.26	2350.79
			305.37	2430.41
			308.15	2639.93
			310.93	2849.44

Table S2: Thermodynamic properties of pure hydrogen in the gas phase from REFPROP.[7]

T/[K]	P/[bar]	α_P/[1/K]	c_P/[J/mol/K]	μ_{JT}/[K/bar]
423.15	50	0.0023186	29.326	-0.046
423.15	80	0.0022919	29.389	-0.047
423.15	100	0.002274	29.429	-0.047
423.15	300	0.0020983	29.727	-0.050
423.15	500	0.0019383	29.907	-0.052
423.15	800	0.0017361	30.067	-0.053
423.15	1000	0.0016237	30.135	-0.053
366.48	10.00	0.0027182	29.164	-0.040
366.48	50.00	0.0026758	29.294	-0.041
366.48	80.00	0.0026433	29.382	-0.042
366.48	100.00	0.0026213	29.437	-0.043
366.48	300.00	0.0023981	29.83	-0.048

Table S3: Chemical potentials of ice and water as a function of temperature and pressure. T_{m} and P_{m} are the melting temperatures and pressures of ice. $\mu_{\mathrm{ice,water}}$ denotes the identical chemical potential of water and ice at equilibrium along the melting line. The molar volumes of ice, $\upsilon_{\mathrm{ice}}(T_{\mathrm{m}}, P_{\mathrm{m}})$, are computed along the melting line using equations 14 to 16.[8] Molar volumes of water, $\upsilon_{\mathrm{water}}(T_{\mathrm{m}}, P_{\mathrm{m}})$, along the melting line are obtained from REFPPROP.[7] ΔP is the difference between the melting pressure P_{m} and pressure P.

T_{m}	P_{m}	$\upsilon_{\mathrm{ice}}(T_{\mathrm{m}}, P_{\mathrm{m}})$	$\upsilon_{\mathrm{water}}(T_{\mathrm{m}}, P_{\mathrm{m}})$	$\mu_{\mathrm{water,ice}} - \mu^0$	P	$\upsilon_{\mathrm{ice}}\Delta P$	$\upsilon_{\mathrm{water}}\Delta P$	$\mu_{\mathrm{ice}}(T_{\mathrm{m}}, P) - \mu^0$	$\mu_{\mathrm{water}}(T_{\mathrm{m}}, P) - \mu^0$
[K]	[bar]	[$10^{-5}\mathrm{m}^3$/mol]		[kJ/mol]	[bar]	[kJ/mol]		[kJ/mol]	
272.4	100	1.961	1.793	-35.35	50	-0.10	-0.09	-35.45	-35.44
272.4	100	1.961	1.793	-35.35	80	-0.04	-0.04	-35.39	-35.38
272.4	100	1.961	1.793	-35.35	100	0.00	0.00	-35.35	-35.35
272.4	100	1.961	1.793	-35.35	200	0.20	0.18	-35.15	-35.17
272.4	100	1.961	1.793	-35.35	300	0.39	0.36	-34.96	-34.99
272.4	100	1.961	1.793	-35.35	400	0.59	0.54	-34.76	-34.81
272.4	100	1.961	1.793	-35.35	500	0.78	0.72	-34.56	-34.63
272.4	100	1.961	1.793	-35.35	600	0.98	0.90	-34.37	-34.45
272.4	100	1.961	1.793	-35.35	700	1.18	1.08	-34.17	-34.27
272.4	100	1.961	1.793	-35.35	800	1.37	1.26	-33.98	-34.09
272.4	100	1.961	1.793	-35.35	900	1.57	1.43	-33.78	-33.91
272.4	100	1.961	1.793	-35.35	1000	1.76	1.61	-33.58	-33.74

Continued on next page

T_m	P_m	$v_{ice}(T_m, P_m)$	$v_{water}(T_m, P_m)$	$\mu_{water,ice} - \mu^0$	P	$v_{ice}\Delta P$	$v_{water}\Delta P$	$\mu_{ice}(T_m, P) - \mu^0$	$\mu_{water}(T_m, P) - \mu^0$
[K]	[bar]	[10^{-5}m^3/mol]		[kJ/mol]	[bar]	[kJ/mol]		[kJ/mol]	
272.4	100	1.961	1.793	-35.35	1100	1.96	1.79	-33.39	-33.56
272.4	100	1.961	1.793	-35.35	1200	2.16	1.97	-33.19	-33.38
272.4	100	1.961	1.793	-35.35	1300	2.35	2.15	-33.00	-33.20
272.4	100	1.961	1.793	-35.35	1400	2.55	2.33	-32.80	-33.02
270.79	300	1.954	1.776	-35.04	50	-0.49	-0.44	-35.52	-35.48
270.79	300	1.954	1.776	-35.04	80	-0.43	-0.39	-35.47	-35.43
270.79	300	1.954	1.776	-35.04	100	-0.39	-0.36	-35.43	-35.39
270.79	300	1.954	1.776	-35.04	200	-0.20	-0.18	-35.23	-35.21
270.79	300	1.954	1.776	-35.04	300	0.00	0.00	-35.04	-35.04
270.79	300	1.954	1.776	-35.04	400	0.20	0.18	-34.84	-34.86
270.79	300	1.954	1.776	-35.04	500	0.39	0.36	-34.64	-34.68
270.79	300	1.954	1.776	-35.04	600	0.59	0.53	-34.45	-34.50
270.79	300	1.954	1.776	-35.04	700	0.78	0.71	-34.25	-34.33
270.79	300	1.954	1.776	-35.04	800	0.98	0.89	-34.06	-34.15
270.79	300	1.954	1.776	-35.04	900	1.17	1.07	-33.86	-33.97
270.79	300	1.954	1.776	-35.04	1000	1.37	1.24	-33.67	-33.79

Continued on next page

T_m	P_m	$v_{ice}(T_m, P_m)$	$v_{water}(T_m, P_m)$	$\mu_{water,ice} - \mu^0$	P	$v_{ice}\Delta P$	$v_{water}\Delta P$	$\mu_{ice}(T_m, P) - \mu^0$	$\mu_{water}(T_m, P) - \mu^0$
[K]	[bar]	$[10^{-5}m^3/mol]$		[kJ/mol]	[bar]	[kJ/mol]		[kJ/mol]	
270.79	300	1.954	1.776	-35.04	1100	1.56	1.42	-33.47	-33.62
270.79	300	1.954	1.776	-35.04	1200	1.76	1.60	-33.28	-33.44
270.79	300	1.954	1.776	-35.04	1300	1.95	1.78	-33.08	-33.26
270.79	300	1.954	1.776	-35.04	1400	2.15	1.95	-32.89	-33.08
269.06	500	1.948	1.759	-34.73	50	-0.88	-0.79	-35.61	-35.52
269.06	500	1.948	1.759	-34.73	80	-0.82	-0.74	-35.55	-35.47
269.06	500	1.948	1.759	-34.73	100	-0.78	-0.70	-35.51	-35.43
269.06	500	1.948	1.759	-34.73	200	-0.58	-0.53	-35.31	-35.26
269.06	500	1.948	1.759	-34.73	300	-0.39	-0.35	-35.12	-35.08
269.06	500	1.948	1.759	-34.73	400	-0.19	-0.18	-34.92	-34.91
269.06	500	1.948	1.759	-34.73	500	0.00	0.00	-34.73	-34.73
269.06	500	1.948	1.759	-34.73	600	0.19	0.18	-34.53	-34.55
269.06	500	1.948	1.759	-34.73	700	0.39	0.35	-34.34	-34.38
269.06	500	1.948	1.759	-34.73	800	0.58	0.53	-34.14	-34.20
269.06	500	1.948	1.759	-34.73	900	0.78	0.70	-33.95	-34.03
269.06	500	1.948	1.759	-34.73	1000	0.97	0.88	-33.76	-33.85

Continued on next page

T_m	P_m	$v_{ice}(T_m, P_m)$	$v_{water}(T_m, P_m)$	$\mu_{water,ice} - \mu^0$	P	$v_{ice}\Delta P$	$v_{water}\Delta P$	$\mu_{ice}(T_m, P) - \mu^0$	$\mu_{water}(T_m, P) - \mu^0$
[K]	[bar]	[10^{-5}m^3/mol]		[kJ/mol]	[bar]	[kJ/mol]		[kJ/mol]	
269.06	500	1.948	1.759	-34.73	1100	1.17	1.06	-33.56	-33.67
269.06	500	1.948	1.759	-34.73	1200	1.36	1.23	-33.37	-33.50
269.06	500	1.948	1.759	-34.73	1300	1.56	1.41	-33.17	-33.32
269.06	500	1.948	1.759	-34.73	1400	1.75	1.58	-32.98	-33.15
267.21	700	1.943	1.743	-34.43	50	-1.26	-1.13	-35.69	-35.56
267.21	700	1.943	1.743	-34.43	80	-1.20	-1.08	-35.63	-35.51
267.21	700	1.943	1.743	-34.43	100	-1.17	-1.05	-35.60	-35.48
267.21	700	1.943	1.743	-34.43	200	-0.97	-0.87	-35.40	-35.30
267.21	700	1.943	1.743	-34.43	300	-0.78	-0.70	-35.21	-35.13
267.21	700	1.943	1.743	-34.43	400	-0.58	-0.52	-35.01	-34.95
267.21	700	1.943	1.743	-34.43	500	-0.39	-0.35	-34.82	-34.78
267.21	700	1.943	1.743	-34.43	600	-0.19	-0.17	-34.62	-34.60
267.21	700	1.943	1.743	-34.43	700	0.00	0.00	-34.43	-34.43
267.21	700	1.943	1.743	-34.43	800	0.19	0.17	-34.24	-34.26
267.21	700	1.943	1.743	-34.43	900	0.39	0.35	-34.04	-34.08
267.21	700	1.943	1.743	-34.43	1000	0.58	0.52	-33.85	-33.91

Continued on next page

T_m	P_m	$v_\mathrm{ice}(T_\mathrm{m}, P_\mathrm{m})$	$v_\mathrm{water}(T_\mathrm{m}, P_\mathrm{m})$	$\mu_\mathrm{water,ice} - \mu^0$	P	$v_\mathrm{ice}\Delta P$	$v_\mathrm{water}\Delta P$	$\mu_\mathrm{ice}(T_\mathrm{m}, P) - \mu^0$	$\mu_\mathrm{water}(T_\mathrm{m}, P) - \mu^0$
[K]	[bar]	[10^{-5}m^3/mol]		[kJ/mol]	[bar]	[kJ/mol]		[kJ/mol]	
267.21	700	1.943	1.743	-34.43	1100	0.78	0.70	-33.65	-33.73
267.21	700	1.943	1.743	-34.43	1200	0.97	0.87	-33.46	-33.56
267.21	700	1.943	1.743	-34.43	1300	1.17	1.05	-33.26	-33.38
267.21	700	1.943	1.743	-34.43	1400	1.36	1.22	-33.07	-33.21
266.73	750	1.942	1.740	-34.36	50	-1.36	-1.22	-35.72	-35.57
266.73	750	1.942	1.740	-34.36	80	-1.30	-1.17	-35.66	-35.52
266.73	750	1.942	1.740	-34.36	100	-1.26	-1.13	-35.62	-35.49
266.73	750	1.942	1.740	-34.36	200	-1.07	-0.96	-35.42	-35.31
266.73	750	1.942	1.740	-34.36	300	-0.87	-0.78	-35.23	-35.14
266.73	750	1.942	1.740	-34.36	400	-0.68	-0.61	-35.04	-34.96
266.73	750	1.942	1.740	-34.36	500	-0.49	-0.43	-34.84	-34.79
266.73	750	1.942	1.740	-34.36	600	-0.29	-0.26	-34.65	-34.62
266.73	750	1.942	1.740	-34.36	700	-0.10	-0.09	-34.45	-34.44
266.73	750	1.942	1.740	-34.36	750	0.00	0.00	-34.36	-34.36
266.73	750	1.942	1.740	-34.36	800	0.10	0.09	-34.26	-34.27
266.73	750	1.942	1.740	-34.36	900	0.29	0.26	-34.06	-34.10

Continued on next page

T_m	P_m	$v_\mathrm{ice}(T_\mathrm{m}, P_\mathrm{m})$	$v_\mathrm{water}(T_\mathrm{m}, P_\mathrm{m})$	$\mu_\mathrm{water,ice} - \mu^0$	P	$v_\mathrm{ice}\Delta P$	$v_\mathrm{water}\Delta P$	$\mu_\mathrm{ice}(T_\mathrm{m}, P) - \mu^0$	$\mu_\mathrm{water}(T_\mathrm{m}, P) - \mu^0$
[K]	[bar]	[10^{-5}m^3/mol]		[kJ/mol]	[bar]	[kJ/mol]		[kJ/mol]	
266.73	750	1.942	1.740	-34.36	1000	0.49	0.43	-33.87	-33.92
266.73	750	1.942	1.740	-34.36	1100	0.68	0.61	-33.68	-33.75
266.73	750	1.942	1.740	-34.36	1200	0.87	0.78	-33.48	-33.57
266.73	750	1.942	1.740	-34.36	1300	1.07	0.96	-33.29	-33.40
266.73	750	1.942	1.740	-34.36	1400	1.26	1.13	-33.09	-33.23
264.21	1000	1.939	1.721	-33.99	50	-1.84	-1.63	-35.84	-35.63
264.21	1000	1.939	1.721	-33.99	80	-1.78	-1.58	-35.78	-35.58
264.21	1000	1.939	1.721	-33.99	100	-1.74	-1.55	-35.74	-35.54
264.21	1000	1.939	1.721	-33.99	200	-1.55	-1.38	-35.55	-35.37
264.21	1000	1.939	1.721	-33.99	300	-1.36	-1.20	-35.35	-35.20
264.21	1000	1.939	1.721	-33.99	400	-1.16	-1.03	-35.16	-35.03
264.21	1000	1.939	1.721	-33.99	500	-0.97	-0.86	-34.96	-34.85
264.21	1000	1.939	1.721	-33.99	600	-0.78	-0.69	-34.77	-34.68
264.21	1000	1.939	1.721	-33.99	700	-0.58	-0.52	-34.58	-34.51
264.21	1000	1.939	1.721	-33.99	800	-0.39	-0.34	-34.38	-34.34
264.21	1000	1.939	1.721	-33.99	900	-0.19	-0.17	-34.19	-34.17

Continued on next page

T_m	P_m	$\upsilon_\mathrm{ice}(T_\mathrm{m}, P_\mathrm{m})$	$\upsilon_\mathrm{water}(T_\mathrm{m}, P_\mathrm{m})$	$\mu_\mathrm{water,ice} - \mu^0$	P	$\upsilon_\mathrm{ice}\Delta P$	$\upsilon_\mathrm{water}\Delta P$	$\mu_\mathrm{ice}(T_\mathrm{m}, P) - \mu^0$	$\mu_\mathrm{water}(T_\mathrm{m}, P) - \mu^0$
[K]	[bar]	$[10^{-5}\mathrm{m}^3/\mathrm{mol}]$		[kJ/mol]	[bar]	[kJ/mol]		[kJ/mol]	
264.21	1000	1.939	1.721	-33.99	1000	0.00	0.00	-33.99	-33.99
264.21	1000	1.939	1.721	-33.99	1100	0.19	0.17	-33.80	-33.82
264.21	1000	1.939	1.721	-33.99	1200	0.39	0.34	-33.61	-33.65
264.21	1000	1.939	1.721	-33.99	1300	0.58	0.52	-33.41	-33.48
264.21	1000	1.939	1.721	-33.99	1400	0.78	0.69	-33.22	-33.31

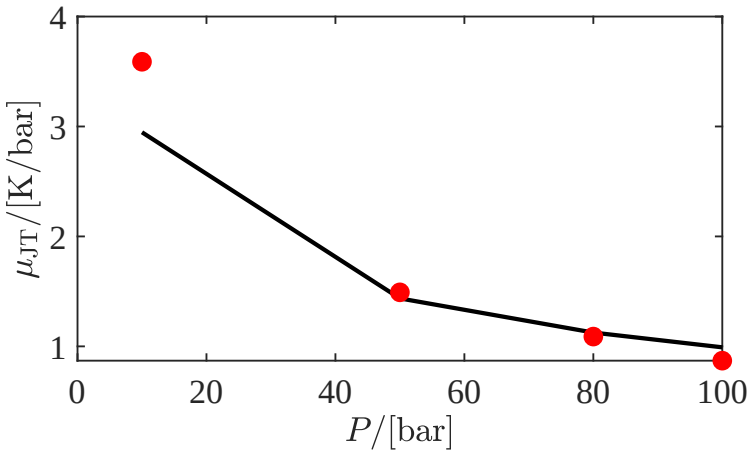

Figure S1: Joule-Thomson coefficient of TIP3P water vapor (circles), and the corresponding result obtained from REFPROP.[7] The calculations are performed along the VLE line of pure water, using experimental vapor densities.

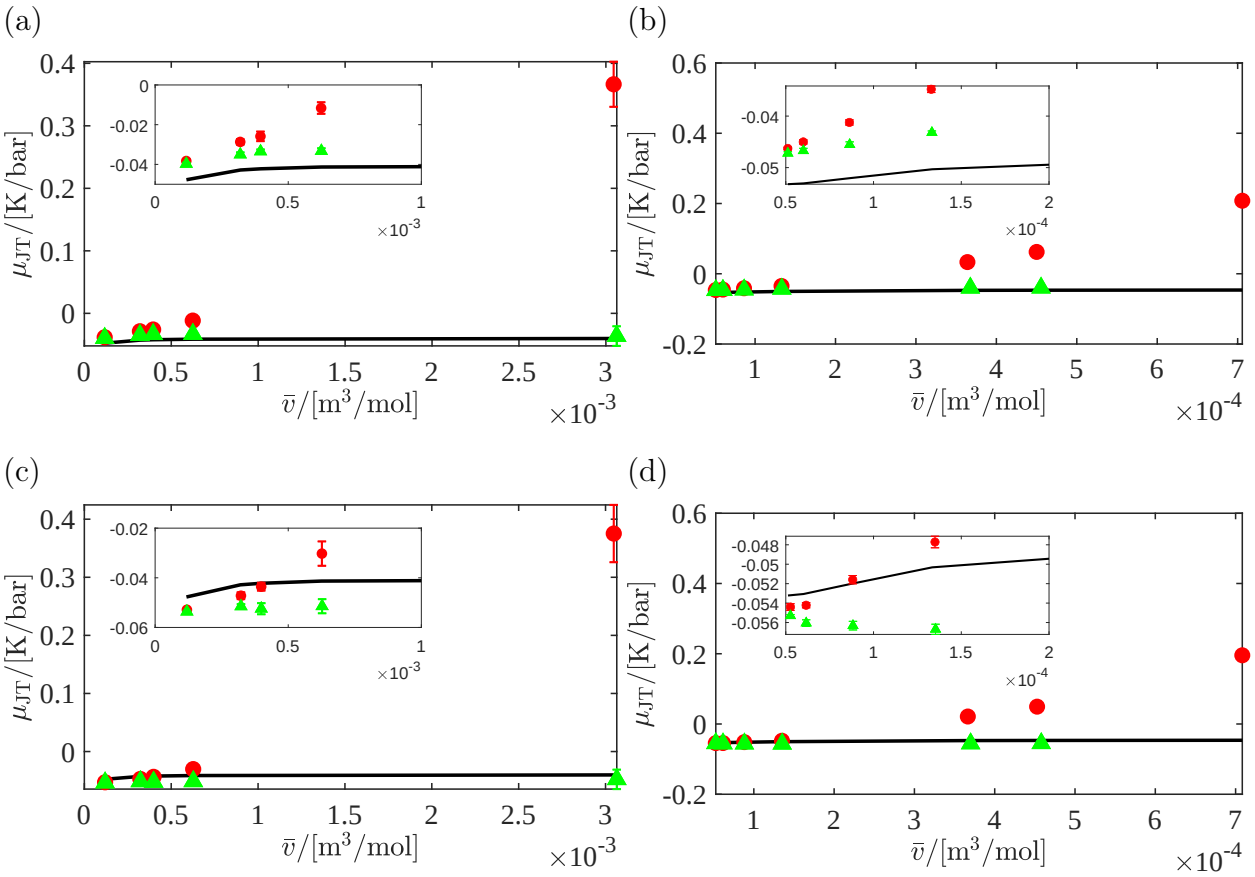

Figure S2: Joule-Thomson coefficients of pure hydrogen in the gas phase, and hydrogen that is saturated with water. (Triangles): pure hydrogen, (circles): hydrogen-water mixtures, (lines): empirical data for pure hydrogen obtained from REFPROP.[7] Joule-Thomson coefficients of mixtures simulated using the TIP3P[9] and Marx[10] force fields are shown in subfigures (a) and (b) for $T = 366$ K and $T = 423$ K, respectively. Joule-Thomson coefficients of mixtures simulated using the TIP3P[9] and Vrabec[11] force fields are shown in subfigures (c) and (d) for $T = 366$ K and $T = 423$ K, respectively The composition in the gas phase is obtained from VLE simulations of water-hydrogen mixture at $T = 423$ K and $T = 366$ K. Raw data (including the composition in the gas phase) are provided in Tables S4 to S6 of this Supporting Information.

S5 Importance of the chemical potential of water in VLE calculations of water-hydrogen mixtures

Among the commonly used force fields of water with fixed point-charges, the TIP4P/2005 force field[12] is one of the best rigid models for liquid water for calculating densities and transport properties.[12,13] For water-hydrogen mixtures at high pressures, it was shown in Ref.[14] that force field combinations with the TIP4P/2005 water model predict hydrogen solubilities in liquid water in good agreement with experiments. However, the solubilities of water in the hydrogen gas phase are noticeably underpredicted compared to experiments.[14] In Ref.,[14] it was shown that at 323.15 K, and pressures in the range of 100 bar to 1000 bar, the chemical potentials for the TIP4P/2005 water model deviate from the IAPWS empirical EoS[7,15] by approximately -500 K in units of energy/k_{B}. This is a significant deviation, which suggests that improvements on the water model may be needed. The TIP3P force field for water predicts the chemical potential of water much better than the TIP4P/2005 force field.[14]

Here, we show that the quality of the water force field for predicting chemical potentials plays an important role in VLE calculations of water-hydrogen systems. This is because the number density of water in the gas phase is directly related to the chemical potential of water in the liquid phase (see Eq. S26). Since the TIP4P/2005 force field is one of the best non-polarizable force fields of water, we make an effort to improve the accuracy of the computed chemical potentials by scaling the charges, and varying the well depth of the Lennard-Jones potential (ϵ_{OO}). The geometry of the water model and the Lennard-Jones size parameters σ are unchanged.[12] Scaling the charges changes the dipole moment of water. The dipole moment of the TIP4P/2005 water model is 2.305 D. The dipole moment of the modified force field with scaling factor of 0.955 is ca. 2.2 D. For every value of the dipole moment, ϵ_{OO} is adjusted such that the chemical potentials (at $T = 323$ K and $P = 100$ bar) are in good agreement with experimental values obtained from REFPROP.[15]

Changes in ϵ_{OO} were performed in steps of 2.5 K in units of energy/k_B. An overview of the scaling factors and modified charges for the modified TIP4P/2005 force field is provided in Table S4. It can be observed from Table S4 that the chemical potential increases with ϵ_{OO} while the density of the liquid water decreases with ϵ_{OO}. To reproduce the value of the chemical potential from REFPROP,[15] we use linear regression on the simulation data in Table S4. For $\epsilon_{OO}/k_B = 79.86$ K, the chemical potential of the modified force field (obtained from simulations in the *NPT* ensemble) is in excellent agreement with the chemical potential obtained from the IAPWS equation of state.[15] To examine the effect of the chemical potential on the VLE of water-hydrogen mixtures, we selected $\epsilon_{OO}/k_B = 79.86$ K and thereby recognizing some loss of accuracy for density predictions. The corresponding charges for the hydrogen and the dummy site of the water model are $q_H = 0.53136$ e, and $q_M = -1.062724$ e, respectively. An overview of the parameters for the TIP4P/2005 force field,[12] the modified TIP4P force field, and the TIP3P force field[9] is provided in Table S5.

To compare the performance of the water force fields in Table S5, VLE calculations in an expanded version of the Gibbs ensemble (with the CFCMC method[16–18]) were performed for pure water. The densities of the liquid and the gas phases, and the chemical potentials of water at equilibrium were compared to experimental values. Simulation details are provided in Ref.[14] The results are shown in Fig. S3, and the raw data are provided in Table S6. For the modified TIP4P force field, it can be observed that on average, the deviation in liquid density from experimental coexistence densities, is reduced by 45% compared to the TIP3P force field, which is quite an improvement. For the liquid coexistence densities, the original TIP4P/2005 force field outperforms the other force fields, but our modified TIP4P is much better than the TIP3P force field. The chemical potentials of the modified TIP4P force field are in excellent agreement with experimental values from the IAPWS equation of state.[15] For the force fields used in Fig. S3, the chemical potentials of water obtained from the TIP4P/2005 force field deviate the most from experimental data. Since one of the conditions of phase equilibrium is equality of chemical potentials in coexisting phases,

any deviation from the actual values of chemical potentials may have consequences for the composition of the coexisting phases at equilibrium, predicted by the model.

To better visualise the performance of different water force fields, the densities of the coexisting gas- and liquid phases are shown in Fig. S4, and the raw data are provided in Table S6. It is clear from Fig. S4 that at low to medium vapor densities, the modified TIP4P force field outperforms the TIP4P/2005 force field. The contribution of the excess chemical potential in the gas phase, at low densities, is very small. This means that the ideal gas contribution of the chemical potential (related to the number density) in the gas phase almost equals the total chemical potential of water in the liquid phase. The results in Fig. S4(a) imply that accurate computations of the chemical potential (*e.g.* using the modified TIP4P force field) leads to accurate densities in the vapor phase at low densities/pressures. The vapor densities at coexistence obtained using the original TIP4P/2005 force field are underpredicted as shown in Fig. S4. The liquid densities at coexistence are however best predicted using the original TIP4P2005 force field. The deviation of densities from experimental data, predicted using the TIP3P and the modified TIP4P force fields increases at lower liquid densities (higher temperatures).

The computed VLEs of water-hydrogen using the modified TIP4P and the Marx force fields are shown in Fig. S5, and the raw data are provided in Table S7. Details on the simulations and the methodology can be found in Ref.[14] In contrast to the solubilities calculated with the original TIP4P/2005 force field in Ref.,[14] the gas phase solubilities of water using the modified TIP4P force field are in excellent agreement with experimental solubilities. The solubilities of hydrogen in the liquid phase are very similar using the TIP4P/2005 and the modified TIP4P force fields. The modified TIP4P force field also outperforms the TIP3P force field for the solubility of hydrogen in liquid water. Given the results provided in Fig. S5, we would like to emphasize the importance of the chemical potential for fitting force field parameters. Due to inherent limitations of rigid force fields with fixed point charges, it was not possible to also obtain accurate coexistence densities of water in the liquid phase. By

comparing the results in Fig. S5 to the results in Ref.,[14] one can observe that the modified TIP4P force field outperforms other force fields in calculating the VLE of water-hydrogen mixtures at high pressures. Further research is needed to obtain force fields that can accurately describe thermodynamic properties of water.

Table S4: Densities and chemical potentials of liquid water for the modified TIP4P/2005 force field at $T = 323.15$ K and $P = 100$ bar. The experimental values for the densities and chemical potentials are obtained from REFPROP.[7] q_{H} and q_{M} indicate the scaled charges of the hydrogen and dummy sites, and μ_{dip} is the dipole moment of the modified force field. The geometry of the TIP4P/2005 force field[12] was used. Numbers in brackets indicate uncertainties in the last digit (95% confidence interval).

Scale factor	q_{H}/[e]	q_{M}/[e]	μ_{dip}/[D]	$\epsilon_{\mathrm{OO}}/k_{\mathrm{B}}$/[K]	$\rho^{\mathrm{sim}}_{\mathrm{H_2O}}$/[kg/m^3]	$\rho^{\mathrm{REFPROP}}_{\mathrm{H_2O}}$/[kg/m^3]	$(\mu^{\mathrm{sim}}_{\mathrm{H_2O}} - \mu^0)/k_{\mathrm{B}}$/[K]	$(\mu^{\mathrm{REFPROP}}_{\mathrm{H_2O}} - \mu^0)/k_{\mathrm{B}}$/[K]
0.960	0.53414	-1.06829	2.213	80.696	984(1)	992.31	-4179(20)	-4112.58
0.960	0.53414	-1.06829	2.213	78.196	988(1)	992.31	-4204(28)	-4112.58
0.960	0.53414	-1.06829	2.213	75.696	993(1)	992.31	-4232(26)	-4112.58
0.960	0.53414	-1.06829	2.213	75.000	994(1)	992.31	-4246(17)	-4112.58
0.955	0.53136	-1.06272	2.201	80.696	980(1)	992.31	-4104(20)	-4112.58
0.955	0.53136	-1.06272	2.201	78.196	985(1)	992.31	-4130 (24)	-4112.58
0.955	0.53136	-1.06272	2.201	75.696	990(1)	992.31	-4162(18)	-4112.58
0.955	0.53136	-1.06272	2.201	75.000	991(1)	992.31	-4176(22)	-4112.58

Table S5: Force field parameters for the water models used in this study. L is the dummy site for four-site models. θ is the angle between atoms OHO, in degrees. For four-site water models, $\varepsilon = 0.5\theta$. A cutoff radius of 12 Å was used for all LJ interactions. Analytic tail corrections and the Lorentz-Berthelot mixing rules were applied.[2,3]

Force Field Parameters	TIP3P[19]	TIP4P/2005[12]	Modified TIP4P (this work)
ϵ_{OO}/k_B/[K]	76.500	93.196	79.86
σ_{OO}/[Å]	3.151	3.1589	3.1589
q_O/[e]	-0.834	-	-
q_H/[e]	0.417	0.5564	0.53136
q_L/[e]	-	-1.1128	-1.06272
r_{OH}/[Å]	0.957	0.9572	0.9572
r_{OL}/[Å]	-	0.1546	0.1546
θ	-	104.52	104.52
φ	-	52.26	52.26

Table S6: Liquid densities, vapor densities and the chemical potentials of water using the modified TIP4P (this work), TIP4P/2005[12] and TIP3P[9] force fields, based on vapor-liquid equilibria from CFCGE simulations between $T = 300$ K to $T = 550$ K. The corresponding empirical results are obtained from REFPROP.[7] Numbers between brackets indicate uncertainties with 95% confidence interval.

T/[K]	ρ_{liq}/[kg/m^3]	ρ_{gas}/[kg/m^3]	$(\mu - \mu^0)$/[K]
Modified TIP4P (this work)			
300	992.3(6)	0.0245(4)	-4208(5)
350	957.5(5)	0.279(6)	-4069(7)
400	907.1(9)	1.51(5)	-4010(11)
450	842.3(3)	5.89(8)	-3971(5)
500	758(1)	18.7(3)	-3974(6)
550	634(1)	55(2)	-4017(5)
TIP4P/2005[12]			
300	996.4(8)	0.0059(3)	-4631(14)
350	971.4(3)	0.083(2)	-4487(9)
400	932.6(3)	0.546(4)	-4394(4)
450	882.2(7)	2.30(4)	-4339(6)
500	820(1)	7.5(1)	-4316(5)
550	739(1)	20.7(4)	-4329(5)
TIP3P[9]			
300	983.2(1)	0.0358(1)	-4097(9)
350	933.9(5)	0.355(6)	-3995(5)
400	871.9(4)	1.84(2)	-3953(4)
450	795.7(9)	6.89(6)	-3944(3)
500	696(1)	22.6(3)	-3965(2)
REFPROP[7]			
300	996.51	0.02559	-4192.47
350	973.7	0.26029	-4084.45
400	937.49	1.3694	-4019.82
450	890.34	4.812	-3991.17
500	831.31	13.199	-3994.82

Table S7: Computed compositions of $H_2O - H_2$ mixtures at coexistence using MC simulations. x_{H_2} is the mole fraction of hydrogen in the liquid phase, y_{H_2O} is the mole fraction of water in the gas phase. The $H_2O - H_2$ mixture is defined by the modified TIP4P force field in this work (Table S5) and Marx[10] force field. The simulation techniques are performed in the CFC Gibbs Ensemble. Simulation details are provided in Ref.[14] σ_x is the uncertainty of x (95% confidence interval).

T/[K]	P/[bar]	x_{H_2}/[−]	$\sigma_{x_{H_2}}$	y_{H_2O}/[−]	$\sigma_{y_{H_2O}}$	Sim. Tech.
323	10	1.4×10^{-4}	1×10^{-5}	1.3×10^{-2}	1×10^{-3}	CFCGE
323	50	7.0×10^{-4}	5×10^{-5}	2.7×10^{-3}	6×10^{-4}	CFCGE
323	80	1.1×10^{-3}	1×10^{-4}	1.7×10^{-3}	5×10^{-4}	CFCGE
323	100	1.4×10^{-3}	1×10^{-4}	1.3×10^{-3}	4×10^{-4}	CFCGE
323	300	3.9×10^{-3}	3×10^{-4}	5×10^{-4}	2×10^{-4}	CFCGE
323	500	6.2×10^{-3}	4×10^{-4}	3×10^{-4}	1×10^{-4}	CFCGE
323	800	9.5×10^{-3}	1×10^{-3}	3×10^{-4}	2×10^{-4}	CFCGE
323	1000	1.1×10^{-2}	1×10^{-3}	2×10^{-4}	1×10^{-4}	CFCGE
366	10	1.6×10^{-4}	1×10^{-5}	8.8×10^{-2}	5×10^{-3}	CFCGE
366	50	8.2×10^{-4}	4×10^{-5}	1.8×10^{-2}	1×10^{-3}	CFCGE
366	80	1.3×10^{-3}	1×10^{-4}	1.1×10^{-2}	1×10^{-3}	CFCGE
366	100	1.6×10^{-3}	1×10^{-4}	9.0×10^{-3}	7×10^{-4}	CFCGE
366	300	4.8×10^{-3}	2×10^{-4}	3.4×10^{-3}	4×10^{-4}	CFCGE
366	500	7.3×10^{-3}	5×10^{-4}	2.2×10^{-3}	4×10^{-4}	CFCGE
366	800	1.2×10^{-2}	1×10^{-3}	1.3×10^{-3}	3×10^{-4}	CFCGE
366	1000	1.3×10^{-2}	1×10^{-3}	1.2×10^{-3}	3×10^{-4}	CFCGE
423	50	1.17×10^{-3}	4×10^{-5}	1.17×10^{-1}	4×10^{-3}	CFCGE
423	80	1.92×10^{-3}	6×10^{-5}	7.3×10^{-2}	3×10^{-3}	CFCGE
423	100	2.40×10^{-3}	9×10^{-5}	6.0×10^{-2}	3×10^{-3}	CFCGE
423	300	7.06×10^{-2}	3×10^{-4}	2.1×10^{-2}	1×10^{-3}	CFCGE
423	500	1.12×10^{-2}	3×10^{-4}	1.3×10^{-2}	8×10^{-4}	CFCGE
423	800	1.62×10^{-2}	6×10^{-4}	8.4×10^{-3}	4×10^{-4}	CFCGE
423	1000	1.96×10^{-2}	7×10^{-4}	6.9×10^{-3}	5×10^{-4}	CFCGE

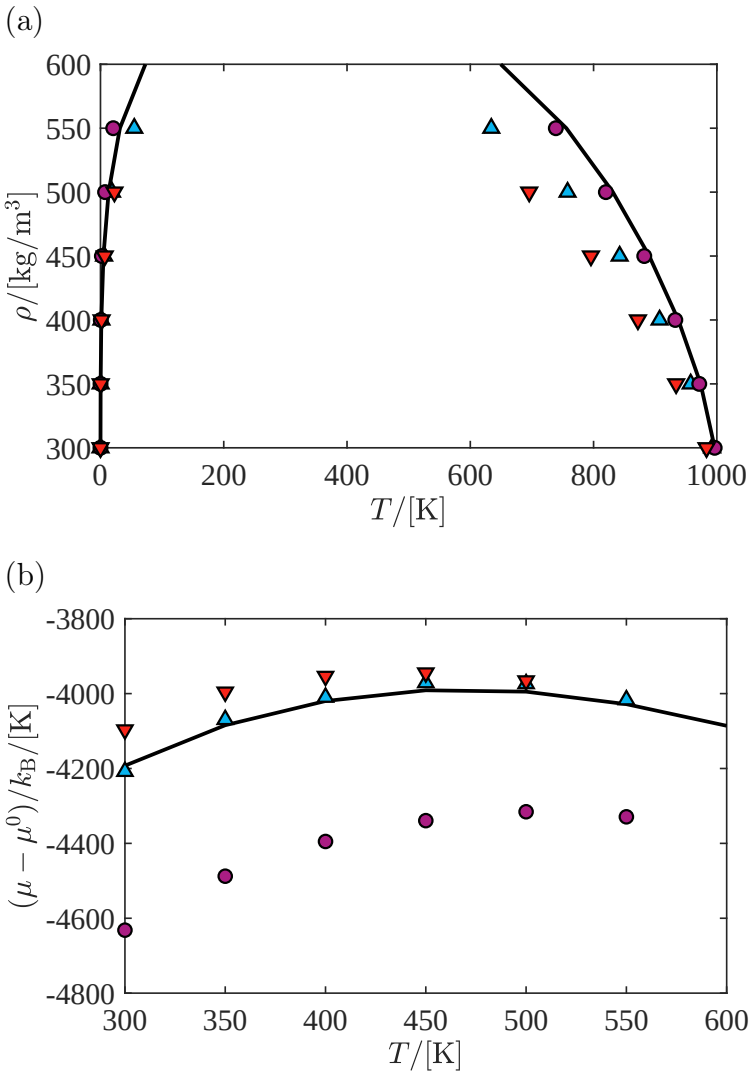

Figure S3: (a): VLE of pure of water using the TIP4P2005[12] (circles), the modified TIP4P (upward-pointing triangles), and the TIP3P[9] force fields (downward-pointing triangles). Lines indicate experimental VLE data obtained from REFPROP.[7,15] (b): Chemical potentials of water along the coexistence line obtained from VLE calculations. The continuous line indicates the chemical potential of water calculated from the IAPWS equation of state in REFPROP.[7,15] Raw data are provided in Table S6.

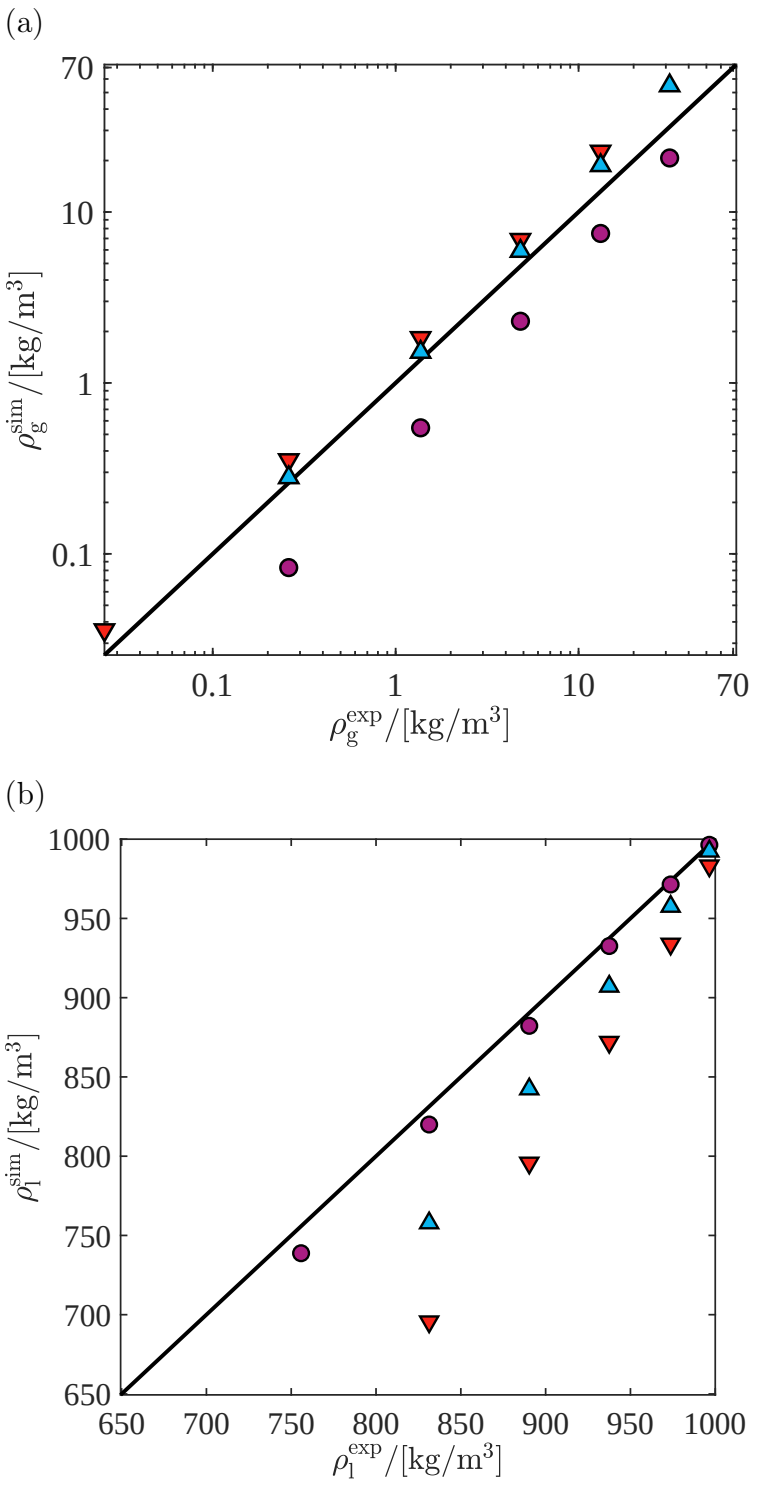

Figure S4: Coexistence densities of (a) vapor and (b) liquid water obtained from the TIP4P2005[12] (circles), the modified TIP4P (upward-pointing triangles), and the TIP3P[9] (downward-pointing triangles) force fields at different temperatures. Lines indicate exact agreement with experimental VLE data obtained from REFPROP.[7,15] Raw data are provided in Table S6.

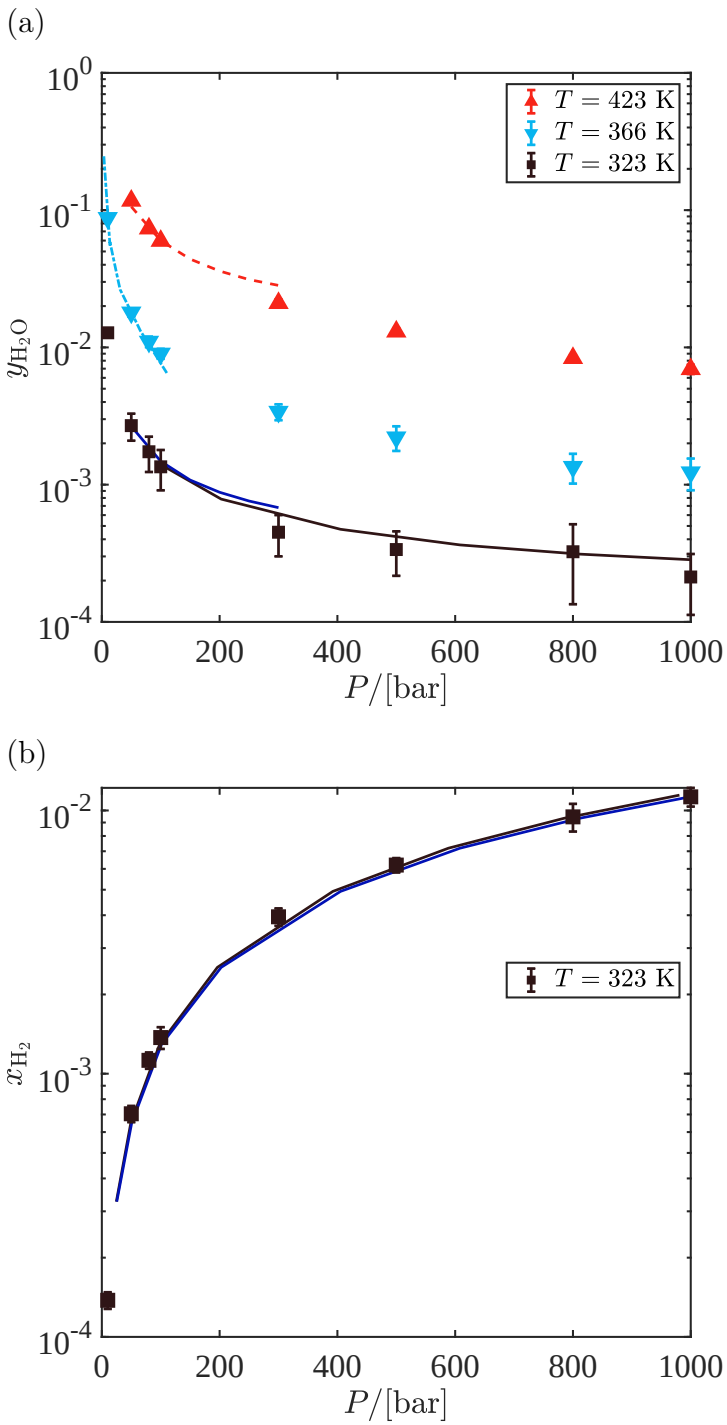

Figure S5: Vapor-Liquid equilibrium of $H_2O - H_2$ (modified TIP4P and Marx[10] force fields) at pressures ranging between $P = 10$ and $P = 1000$ bar. (a): y_{H_2O} in the gas phase and (b): x_{H_2} in the liquid phase. Experiential data in the gas phase for $T = [423, 366, 323]$ K are shown with dashed lines, dash-dot lines, solid lines, respectively.[20–24] Published high pressure data for the liquid phase are only available for $T = 323$ K.[21,25] In Ref.,[14] a detailed overview of available experimental VLE and solubility data for $H_2O - H_2$ systems at high pressures is provided. Error bars are based on uncertainties with 95% confidence interval. Raw data are provided in Table S7.

Literature Cited

(1) Lagache, M.; Ungerer, P.; Boutin, A.; Fuchs, A. H. Prediction of thermodynamic derivative properties of fluids by Monte Carlo simulation. *Phys. Chem. Chem. Phys.* **2001**, *3*, 4333–4339.

(2) Frenkel, D.; Smit, B. *Understanding Molecular Simulation: From Algorithms to Applications*, 2nd ed.; Academic Press: San Diego, California, 2002.

(3) Allen, M. P.; Tildesley, D. J. *Computer Simulation of Liquids*, 2nd ed.; Oxford University Press: Oxford, United Kingdom, 2017.

(4) Moran, M. J.; Shapiro, H. N. *Fundamentals of Engineering Thermodynamics*, 5th ed.; John Wiley & Sons: West Sussex, United Kingdom, 2006.

(5) Sandler, S. I. *Chemical, Biochemical, and Engineering Thermodynamics*, 4th ed.; John Wiley & Sons: Hoboken, N.J., USA, 2006.

(6) Dickinson, H. C.; Osborne, N. S. *Specific heat and heat of fusion of ice*, 1st ed.; Bulletin of the Bureau of Standards 248; US Department of Commerce, Bureau of Standards, 1916.

(7) Lemmon, E. W.; Huber, M. L.; McLinden, M. O. NIST reference fluid thermodynamic and transport properties–REFPROP. *NIST standard reference database* **2002**, *23*, v7, `https://www.nist.gov/srd/refprop`. Accessed: 07-01-2021.

(8) Marion, G.; Jakubowski, S. The compressibility of ice to 2.0 kbar. *Cold Reg. Sci. Technol.* **2004**, *38*, 211 – 218.

(9) Jorgensen, W. L.; Chandrasekhar, J.; Madura, J. D.; Impey, R. W.; Klein, M. L. Comparison of simple potential functions for simulating liquid water. *J. Chem. Phys.* **1983**, *79*, 926–935.

(10) Marx, D.; Nielaba, P. Path-integral Monte Carlo techniques for rotational motion in two dimensions: quenched, annealed, and no-spin quantum-statistical averages. *Phys. Rev. A* **1992**, *45*, 8968–8971.

(11) Köster, A.; Thol, M.; Vrabec, J. Molecular models for the hydrogen age: hydrogen, nitrogen, oxygen, argon, and water. *J. Chem. Eng. Data* **2018**, *63*, 305–320.

(12) Abascal, J. L. F.; Vega, C. A general purpose model for the condensed phases of water: TIP4P/2005. *J. Chem. Phys.* **2005**, *123*, 234505.

(13) Tsimpanogiannis, I. N.; Moultos, O. A.; Franco, L. F. M.; de M. Spera, M. B.; Erdős, M.; Economou, I. G. Self-diffusion coefficient of bulk and confined water: a critical review of classical molecular simulation studies. *Mol. Simul.* **2019**, *45*, 425–453.

(14) Rahbari, A.; Brenkman, J.; Hens, R.; Ramdin, M.; van den Broeke, L. J. P.; Schoon, R.; Henkes, R.; Moultos, O. A.; Vlugt, T. J. H. Solubility of water in hydrogen at high Pressures: a molecular simulation study. *J. Chem. Eng. Data* **2019**, *64*, 4103–4115.

(15) Wagner, W.; Pruß, A. The IAPWS formulation 1995 for the thermodynamic properties of ordinary water substance for general and scientific use. *J. Phys. Chem. Ref. Data* **2002**, *31*, 387–535.

(16) Rahbari, A.; Hens, R.; Ramdin, M.; Moultos, O. A.; Dubbeldam, D.; Vlugt, T. J. H. Recent advances in the continuous fractional component Monte Carlo methodology. *Mol. Simulation* **2020**, In press. doi:10.1080/08927022.2020.1828585.

(17) Hens, R.; Rahbari, A.; Caro-Ortiz, S.; Dawass, N.; Erdős, M.; Poursaeidesfahani, A.; Salehi, H. S.; Celebi, A. T.; Ramdin, M.; Moultos, O. A.; Dubbeldam, D.; Vlugt, T. J. H. Brick-CFCMC: Open Source Software for Monte Carlo Simulations of Phase and Reaction Equilibria Using the Continuous Fractional Component Method. *J. Chem. Inf. Model.* **2020**, *60*, 2678–2682.

(18) Poursaeidesfahani, A.; Torres-Knoop, A.; Dubbeldam, D.; Vlugt, T. J. H. Direct free energy calculation in the Continuous Fractional Component Gibbs ensemble. *J. Chem. Theory Comput.* **2016**, *12*, 1481–1490.

(19) Mark, P.; Nilsson, L. Structure and dynamics of the TIP3P, SPC, and SPC/E water models at 298 K. *J. Phys. Chem. A* **2001**, *105*, 9954–9960.

(20) Maslennikova, V. Y.; Goryunova, N.; Subbotina, L.; Tsiklis, D. The solubility of water in compressed hydrogen. *Russian Journal of Physical Chemistry* **1976**, *50*, 240–243.

(21) Bartlett, E. P. The concentration of water vapor in compressed hydrogen, Nitrogen and a mixture of these gases in the presence of condensed water. *J. Amer. Chem. Soc.* **1927**, *49*, 65–78.

(22) Ugrozov, V. V. Equilibrium compositions of vapor-gas mixtures over solutions. *Russ. J. Phys. Chem.* **1996**, *70*, 1240–1241.

(23) Gillespie, P.; Wilson, G. *Vapor-liquid Equilibrium Data on Water-substitute Gas Components:* N_2-H_2O*,* H_2-H_2O*,* CO-H_2O*,* H_2-CO-H_2O*, and* H_2S-H_2O, 1st ed.; Research report; Gas Processors Association: Provo, Utah, 1980.

(24) Devaney, W.; Berryman, J. M.; Kao, P.-L.; Eakin, B. *High temperature V-L-E measurements for substitute gas components*; 1978; pp 1–27.

(25) Wiebe, R.; Gaddy, V. L. The solubility of hydrogen in water at 0, 50, 75 and 100° from 25 to 1000 atmospheres. *J. Amer. Chem. Soc.* **2005**, *56*, 76–79.